Waters™

Synthetic mRNA Oligo-Mapping Using Ion-Pairing Liquid Chromatography and Mass Spectrometry

Maissa M. Gaye, Jonathan Fox, Johannes P.C. Vissers, Ian Reah, Chris Knowles, Matthew A. Lauber

Waters Corporation

Abstract

Messenger RNA has quickly become an important modality for human medicine, as shown with its evaluation for cancer treatment and the FDA approval of mRNA vaccines for COVID-19. The rapid development of mRNA vaccines and other classes of mRNA therapeutics is supported by advances in analytical methodologies. One important aspect of such methodologies is confirming the identity, purity, and modification(s) of a therapeutic mRNA through mapping its sequence by liquid chromatography-mass spectrometry (LC-MS). Mass spectrometry-based sequencing of RNAs has an advantage over templated RNA sequencing by offering direct molecular detection of fragments, which can be used to localize nucleoside impurities and identify important structural attributes (5'-cap and poly-A tail). As such, we propose a workflow for comprehensive bottom-up LC-UV-MS characterization of mRNAs that yields mRNA component-annotated chromatograms derived from accurate-mass matching.

Benefits

- High chromatographic resolution and MS sensitivity with the use of ion-pairing reversed-phase chromatography in combination with the ACQUITY™ Premier Oligonucleotide BEH™ C_{18} 300 Å Column

- ·Automated mRNA digest annotation based on accurate-mass matching as facilitated by *in silico* mRNA digestion calculations and application of waters_connect/UNIFI™ Scientific Libraries

Introduction

The SARS-CoV-2 pandemic provided the impetus for the fast-paced development of nucleic-acid based medicine, especially synthetic mRNA.[1] Now, 40 years after its discovery in 1961 by Brenner *et al*.[2] [i], mRNA has evolved into being an important modality with massive potential, as shown with the start of an in-human clinical trial for cancer treatment[1–3] and the full approval of two COVID-19 mRNA vaccines by the US Food and Drug Administration in August 2021 and in January 2022, respectively. The rapid development of mRNA vaccines and other classes of mRNA therapeutics are supported by advances in analytical methodologies. One important aspect of such methodologies is confirming the identity, purity, and modification of a therapeutic mRNA through oligo-mapping and sequencing via liquid chromatography hyphenated to mass spectrometry (LC-MS). Nucleic acid sequencing technologies, like Sanger and next-generation sequencing (NGS), provide valuable information to drug developers. However, there is also a heightened level of analysis that can be achieved through the use of LC in combination with tandem MS (LC-MS/MS)[4] or MS^E (alternating low and high collision energy)[5] based fragmentation. Similar to a proteomics bottom-up approach, LC-MS/MS or MS^E based sequencing have the advantage of direct molecular detection of RNA fragments, including the detection and localization of nucleoside impurities and important structural attributes, like lipidated nucleobases,[6] endcapped residues, and polyA tail modifications.[4,7] Unlike bottom-up proteomics workflows, where a plethora of data processing solutions exist, options for RNA mapping are limited. We propose a workflow for oligo-mapping based on a bottom-up approach for the characterization of a given synthetic mRNA within a single platform comprising LC, UV detection and MS measurements. Digestion components were processed using an in-house developed, freely available *in silico* digestion library calculator, mRNAcalcondemand, in combination with waters_connect™ to yield an annotated chromatogram. Here, we demonstrate this analytical approach for mRNA sequence mapping using RNase T1 digested luciferase mRNA.

Experimental

Sample Information

Approximately 90 µg of synthetic Cypridina luciferase mRNA (uncapped and not modified with a polyA tail); a gift from Bijoyita Roy (New England Biolabs, Ipswich, MA) was digested using 3'-guanosine specific ribonuclease RNaseT1 (Worthington Biochemical Corporation, Lakewood, NJ). Note that this workflow was repeated using 10 µg of TriLink Biotechnologies (CleanCap® FLuc mRNA, San Diego, CA) firefly luciferase mRNA (untranslated sequences are proprietary) and comparable results were achieved. Luciferase mRNA was denatured prior to digestion using 20 µL urea (8 M) prepared in nuclease-free buffer (10 mM Tris, 0.1 mM EDTA, pH 7.5 in water, Integrated DNA Technologies, Inc, Coralville, IA) at 80 °C for 5 minutes. Next, 24 µg (~10kU) of RNase T1 (Worthington Biochemical Corporation, Lakewood, NJ) resuspended in nuclease-free buffer was added to the denatured mRNA at room temperature and the mixture was then incubated at 37 °C for 30 minutes. Nuclease-free buffer (40 µL) was added at the end of the incubation period, bringing the total sample volume to 80 µL. The final aliquot was transferred to a polypropylene 300 µL autosampler vial (p/n: 186002639 < https://www.waters.com/nextgen/global/shop/vials-containers--collection-plates/186002639-polypropylene-12-x-32-mm-screw-neck-vial-with-cap-and-preslit-pt.html>). The resulting digest was subjected to ion-pairing reversed-phase chromatography (IP-RPLC) without any further manipulation prior to MS detection in negative ion mode using the BioAccord™ RDa™ Detector.

LC Conditions

LC system:	ACQUITY UPLC™ Premier BSM System (as part of the BioAccord System)
Detector:	ACQUITY UPLC TUV Detector
Wavelength:	260 nm
Column:	ACQUITY Premier Oligonucleotide BEH C18, 2.1 X 150 mm, 300 Å, 1.7 µm (p/n:186010541)
Column Temperature:	70 ˚C
Sample Temperature:	4 ˚C

Injection:	5 µL

Flow Rate:	0.4 mL/min

Mobile phase A	0.1% N,N-diisopropylethylamine (DIPEA) as the IP reagent and 1% 1,1,1,3,3,3-hexafluoroisopropanol (HFIP) in deionized water

Mobile phase B	0.0375% DIPEA and 0.075% HFIP in 65:35 acetonitrile/water

Gradient Table

Time (min)	mL/min	A (%)	B (%)	Curve
Initial	0.4	97	3	*
60	0.4	70	30	6
60.5	0.4	5	95	6
61	0.4	97	3	6
70	0.4	97	3	6

Run time = 70 minutes

MS Conditions

MS system:	BioAccord LC-MS System

Detector:	ACQUITY RDa Detector

Mode:	Full scan with fragmentation

Polarity:	Negative
Cone voltage:	40 V
Fragmentation cone voltage:	80–200 V
Mass range:	High (400–5000 m/z)
Scan rate:	2 Hz
Capillary voltage:	0.80 kV
Desolvation temperature:	400 °C

Results and Discussion

Ion-pairing reversed-phase chromatography (IP-RPLC) with a C_{18} stationary phase has become a tried-and-true approach for the analysis of oligonucleotides.[4,7] The mobile phase contains an ion pairing reagent, commonly an alkylamine, which adsorbs onto the C_{18} stationary phase[8,9,10] and thereby introduces a mixed mode like retention mechanism.[8–10] The N,N-diisopropylethylamine (DIPEA)/ 1,1,1,3,3,3-hexafluoroisopropanol (HFIP) mobile phase system used in this application is compatible with both optical UV detection and negative ion mode mass spectrometry.[4,7,–10] HFIP is used to enhance electrospray ionization.[8]

RNase T1 digested luciferase mRNA was injected onto an ACQUITY Premier Oligonucleotide BEH C_{18} (2.1 x 150 mm, 300 Å, 1.7 μm) Column and gradients were developed with an ACQUITY Premier Binary LC equipped with an ACQUITY UPLC TUV Detector. The ACQUITY Premier Oligonucleotide BEH C_{18} Column used in this work is similar to ACQUITY Premier Oligonucleotide BEH C_{18} 130 Å Column, but with a wider pore size, providing better resolution for longer oligonucleotide species. Data were acquired in triplicate using negative ion mode mass spectrometry with the ACQUITY RDa Detector of a BioAccord Benchtop LC-MS system. Moreover, the ACQUITY RDa Detector was programmed to acquire MS[E] data such that every other scan produced a high energy

fragment ion spectrum that could be later used to corroborate LC peak identifications. Figure 1 depicts total ion chromatograms (TIC) for an RNase T1 control sample (top trace), mRNA control sample (bottom trace) and the digested mRNA (middle trace). Oligonucleotide fragments resulting from the digestion of luciferase mRNA with RNase T1 were readily separated according to a separation with a 4-sigma peak capacity of 613. Overall, chromatographic peaks were sharp and symmetrical with ~0.01 minutes variation in retention time (RT) over triplicate injections. Digest components eluted between 2 and 23 minutes on a 60 minute gradient time method; some incompletely digested mRNA was seen to elute around 29 minutes and intact RNaseT1 eluted around 54 minutes. As can be seen on the top trace of Figure 1, an RNase T1 control sample showed signal only after a 50 minute retention time. This confirmed that RNase T1 would not introduce interference within the retention window of the mRNA digestion components. (Figure 1, middle trace). Likewise, the bottom trace of Figure 1 shows that intact luciferase mRNA elutes at approximately 38 minutes, confirming that the peak observed at 29 minutes in the digested sample (Figure 1, middle trace) corresponds to incompletely digested mRNA. We note here that in the case of synthetic mRNA comprising 5'-cap and poly-A tail structures, peaks at ~29 and 37 minutes are observed post digestion. The slight shift from ~38 minutes to ~37 minutes might be indicative of the undigested polyA structure (an investigation into this chromatographic behavior will be described in a future application note).
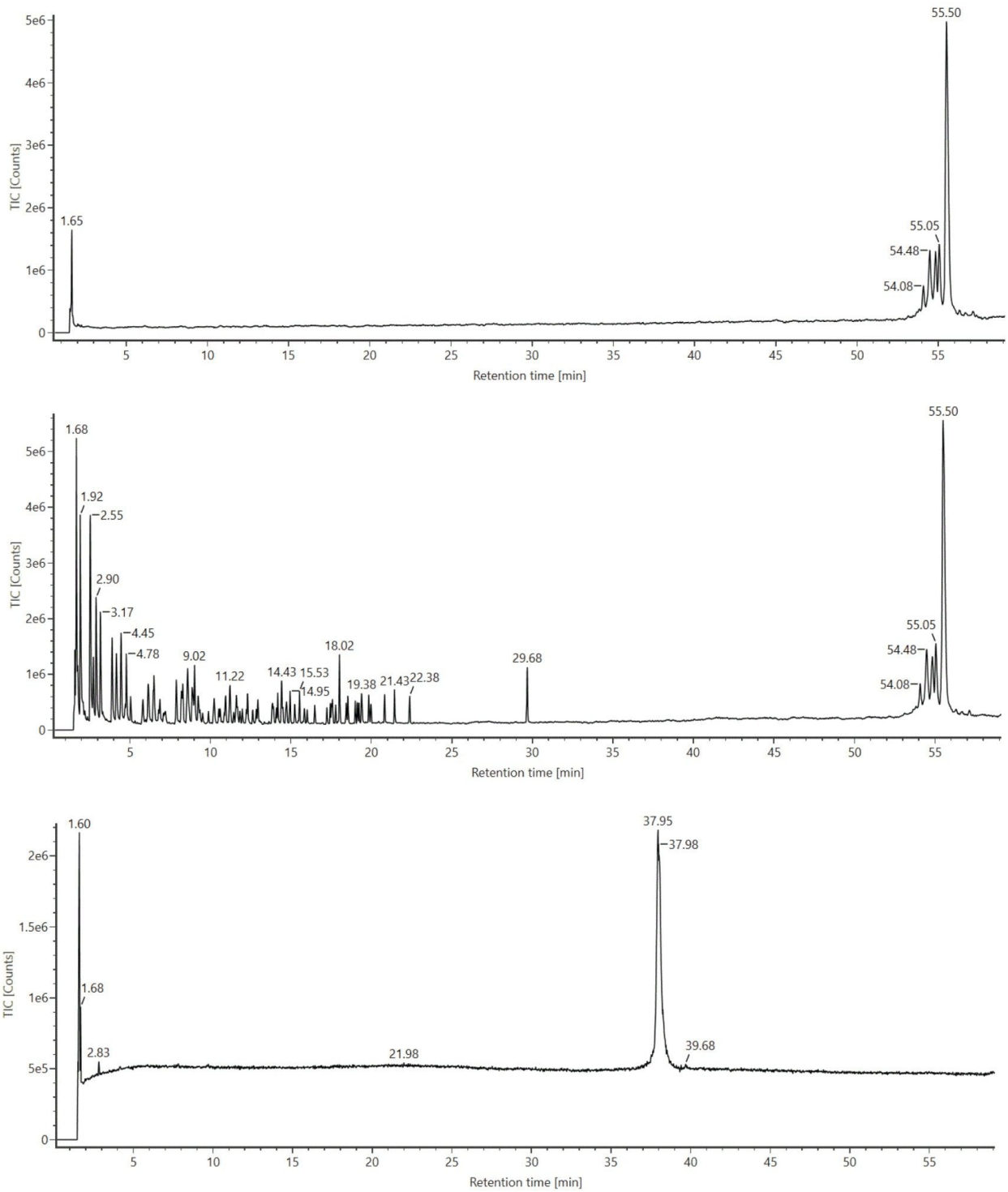
Figure 1: TIC for RNase T1 control sample (top trace), mRNA control sample (bottom trace) and the digest

(middle trace) obtained from ion-pairing reversed-phase chromatography (IP-RPLC) of luciferase mRNA digested with Rnase T1 and analyzed using the ACQUITY UPLC I-Class System (ACQUITY Premier Oligonucleotide BEH C$_{18}$ Column, 2.1 x 150 mm, 300 Å, 1.7 μm) and the BioAccord ACQUITY RDa Detector in negative ion mode.

The graphical user interface (GUI) of the *in-silico* digestion mRNA calculator, mRNAcalcondemand, is shown in Scheme 1. Next to the base sequence, a number of digestion parameters are specified, such as modification(s), enzyme, and missed cleavages. Based on this input, the calculator defaults to a number of MS specific settings, including charge state and *m/z* ranges, as well as the ability to conduct calculations based on monoisotopic or average mass. The generated output, in the form of a flat text csv file, can be utilized in UNIFI or waters_connect software, or used for complementary downstream analysis.

Scheme 1: mRNA calculator GUI for in silico mRNA digest mass calculation.

Next, a library was created where the digest components are considered to be individual analytes, which was achieved by importing the output of the calculator as a spreadsheet into a UNIFI Scientific Library. The created libraries can be utilized in an HRMS Screening Analysis Method, targeting the digest compounds post-acquisition, using user-specified tolerances. The use of mass tolerance-based library matching is demonstrated below. As a result of the library search, an annotated chromatogram is automatically generated (Figure 2). A close-up, corresponding to a zoomed view of the 17 to 20 minute retention time window is represented in Figure

2.
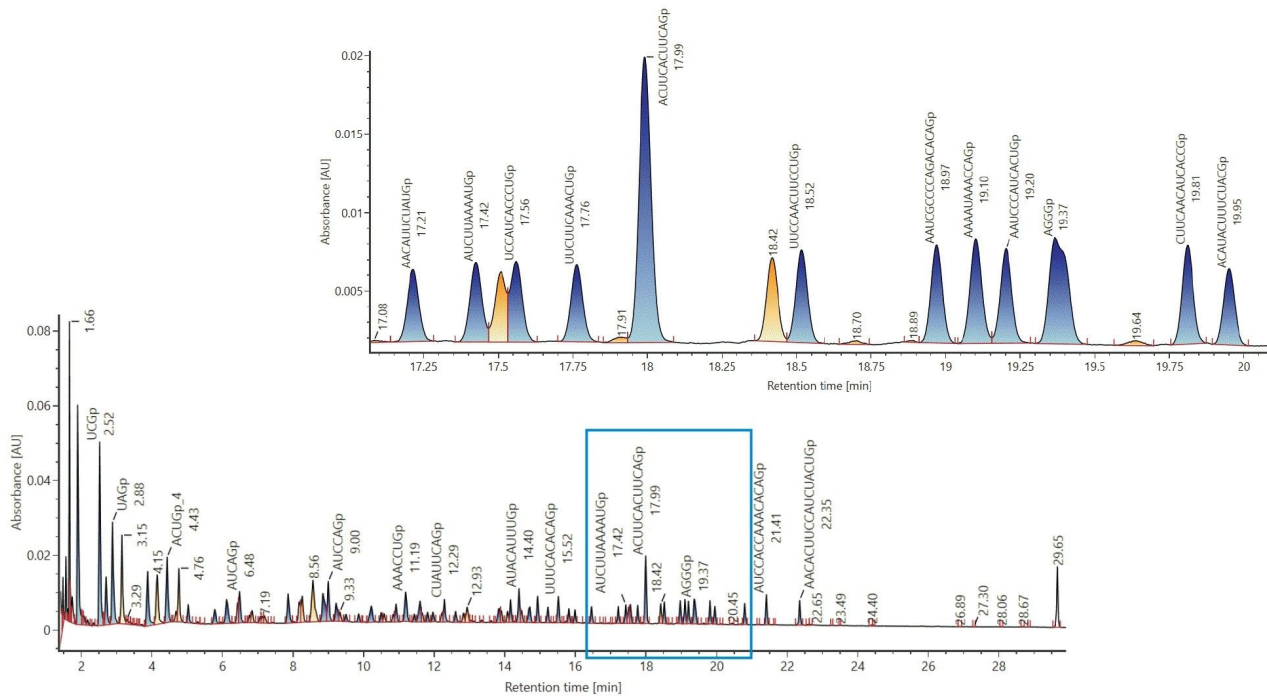
Figure 2: Annotated TIC of luciferase mRNA digest generated after matching, based on accurate mass, to a target component library. Luciferase mRNA was digested with Rnase T1 and analyzed using the ACQUITY Premier BSM LC (ACQUITY Premier Oligonucleotide BEH C_{18} Column, 2.1 x 150 mm, 300 Å, 1.7 μm) and the BioAccord ACQUITY RDa Detector in negative mode. Target components were calculated using the mRNA MASS calculator.

A total of 436, 428, and 441 potential identifications (IDs) of digestion components were produced from each technical replicate upon screening data against an *in silico* library created with an allowance for up to 2 missed cleavages. Several criteria were considered for manual validation. 40 out of 441 identified components were rejected based on abundance and peak shape, *e.g.*, low abundant chromatographic peak shoulders. The majority of these rejected IDs (27 out of 40) were situated between 24 and 60 minutes. Overall, ~60% of the identified and validated components were within 10 ppm mass error (261 digest components). The RNase T1 control sample (Figure 1, top trace) was subjected to the same query and as expected did not yield any identifications. In addition to peak shape and abundance, we further validated the results based on high-confidence interpretation

of isotopic distributions to deduce charge assignments, which yielded 139 digest components (65% within 5 ppm mass error). Lastly, some assignments were not included in the analysis because they appeared to be redundant assignments triggered by repeated detection on broadened and shoulder-containing chromatographic peaks. The number of identifications was thereby reduced by another 16 components. In a couple instances, however, analyte masses showed up at multiple retention times to produce two unique IDs corresponding to two distinct, well-defined chromatographic peaks. Here, we also took note of the presence of isomeric IDs (species having the same chemical composition but different sequences) as well as isobaric IDs (species having different chemical compositions [different exact mass], yet similar nominal mass). Ultimately, 90 unique components could be identified based on accurate-mass matching, and these are reported in Table 1, including isomeric nucleotide sequences and isobaric ions (cells highlighted in grey in Table 1).

Component name	Formula	Observed RT (min)	Neutral mass (Da)	Observed m/z	Charge	Mass error (ppm)	Additional ions observed
UGUGp_1	C38H48N14O31P4	1.64	1320.15604	659.0689	−2	−4	−2H, −H
CCUUCUGCCGp	C92H120N32O73P10	1.65	3150.40375	1049.1302	−3	0.4	−3H
UCUACUGCGp	C84H107N30O66P9	1.7	2870.35772	1434.1633	−2	−6.3	−2H
CCGGUCAAAGp	C96H121N41O69P10	1.93	3261.45959	1086.1526	−3	3.9	−3H
GAAGp	C40H50N20O27P4	2.1	1366.21047	682.0924	−2	−9.2	−2H
CCGp_6	C28H38N11O22P3	2.54	973.14057	485.567	−2	6.6	−2H, −H
GAGACACCCUAGp	C115H145N49O82P12	2.54	3895.55339	1297.5089	−3	−3.2	−3H
CUCGGp	C47H61N18O37P5	2.55	1624.21331	1623.2076	−1	1	−H
CUGp	C28H37N10O23P3	2.55	974.12459	973.1177	−1	0.4	−H, −2H
GAGACAUCAUUGp	C115H143N47O84P12	2.55	3897.52142	1298.1735	−3	3.5	−3H
UAUUGAUAGCAGp	C115H142N46O85P12	2.55	3898.50544	1948.2401	−2	−3.1	−2H
ACGp	C29H38N13O21P3	2.73	997.1518	996.1407	−1	−3.8	−H, −2H
CAGp	C29H38N13O21P3	2.73	997.1518	996.1407	−1	−3.8	−H, −2H
AUGp	C29H37N12O22P3	2.92	998.13582	997.1285	−1	0	−H, −2H
AAGp_4	C30H38N15O20P3	3.18	1021.16304	1020.153	−1	−2.7	−H, −2H
ACACCCUAGAAGp	C115H145N49O81P12	3.44	3879.55848	1292.17	−3	−8.8	−3H, −6H, −9H
UGAUCUUGp	C75H94N26O60P8	3.9	2566.30045	1282.1387	−2	−3.9	−2H
CCCGp	C37H50N14O29P4	3.91	1278.18186	638.0888	−2	6.9	−2H, −3H, −H
CCUGp	C37H49N13O30P4	3.91	1279.16587	638.5822	−2	9	−2H, −3H, −H
CUCUGGGUGp	C75H95N27O60P8	3.91	2581.31135	1289.6535	−2	3.4	−2H
GGUCCCUGp	C75H96N28O59P8	3.91	2580.32733	1289.1652	−2	6.2	−2H
AAGCCGUGp	C77H97N33O56P8	4.17	2627.36578	1312.675	−2	−1.1	−2H
UAAGp_1	C39H49N17O28P4	4.79	1327.18834	1326.1802	−1	−0.7	−H, −2H, −3H
AAAGp	C40H50N20O26P4	5.06	1350.21556	1349.2049	−1	−2.5	−H, −2H, −3H
CUCUGp	C46H60N15O38P5	5.81	1585.19118	791.5962	−2	9	−2H, −3H, −H
UCCCGp	C46H61N16O37P5	5.83	1584.20716	791.1011	−2	5.1	−2H, −3H, −H
CACCGp	C47H62N19O35P5	6.18	1607.23438	802.6146	−2	4.8	−2H, −3H, −H
AUCUGp	C47H60N17O37P5	6.51	1609.20241	803.6021	−2	9.2	−2H, −3H, −H
AUCCGp	C47H61N18O36P5	6.53	1608.21839	803.1076	−2	6.1	−2H, −3H, −H
AAAAACAUGUUGCCGp	C144H179N60O103P15	6.52	4860.66775	1619.2101	−3	−4.7	−3H
CAAAGp	C49H62N23O33P5	6.79	1655.25684	826.625	−2	3.7	−2H, −3H, −H
CCUCUGp	C55H72N18O45P6	7.89	1890.23246	944.1145	−2	5.1	−2H, −3H, −4H, −H
CUCCCGp	C55H73N19O44P6	7.91	1889.24845	943.6212	−2	3.7	−2H, −3H, −4H, −H
CCCCAGp	C56H74N22O42P6	8.29	1912.27566	955.1342	−2	3	−2H, −3H, −4H, −H
AUCCAGp	C57H73N23O42P6	8.58	1937.27091	967.6315	−2	2.6	−2H, −3H, −4H, −H
CAUUAGp	C57H72N22O43P6	8.58	1938.25493	1937.2514	−1	1.9	−H
AUUCUGp	C56H71N19O45P6	8.63	1915.22771	956.614	−2	6.9	−2H, −3H, −4H, −H
AAUCAGp	C58H73N25O41P6	8.88	1961.28215	979.6375	−2	3	−2H, −3H, −4H, −H
UACAAGp	C58H73N25O41P6	8.88	1961.28215	979.6375	−2	3	−2H, −3H, −4H, −H
AUCCAGp	C57H73N23O42P6	8.89	1937.27091	967.6353	−2	6.5	−2H, −3H, −H
AACCUGp	C57H73N23O42P6	9.03	1937.27091	967.634	−2	5.2	−2H, −3H, −4H, −H
ACACAGp	C58H74N26O40P6	9.26	1960.29813	979.1457	−2	3.2	−2H, −3H, −4H, −H
ACAAAGp	C59H74N28O39P6	9.52	1984.30936	991.1508	−2	2.7	−2H, −3H, −4H, −H
UCUUCUGp	C64H82N19O54P7	9.89	2197.24178	1097.6182	−2	3.5	−2H, −3H, −4H
AUCUCUGp	C65H83N22O52P7	10.23	2220.269	1109.1359	−2	7.1	−2H, −3H, −4H
UCUACUGp	C65H83N22O52P7	10.23	2220.269	1109.1359	−2	7.1	−2H, −3H, −4H
UCUACUGp	C65H83N22O52P7	10.61	2220.269	1109.1302	−2	2	−2H, −3H, −4H
AUUCCAGp	C66H84N25O50P7	10.53	2243.29621	1120.643	−2	1.2	−2H, −3H, −4H
CAUACUGp	C66H84N25O50P7	10.53	2243.29621	1120.643	−2	1.2	−2H, −3H, −4H
CAUACUGp	C66H84N25O50P7	10.96	2243.29621	1120.6441	−2	2.2	−2H, −3H, −4H
AUUUCAGp	C66H83N24O51P7	10.95	2244.28023	1121.141	−2	6.6	−2H, −3H, −4H, −H
AAACCUGp	C67H85N28O48P7	11.22	2266.32343	1132.1603	−2	4.5	−2H, −3H, −4H, −H
ACUACAGp	C67H85N28O48P7	11.22	2266.32343	1132.1603	−2	4.5	−2H, −3H, −4H, −H
CCACAAGp	C67H86N29O47P7	11.25	2265.33942	1131.6655	−2	2	−2H, −3H, −4H
UCUCUUCGp	C73H94N22O61P8	11.69	2502.28307	1250.1365	−2	1.1	−2H, −3H, −4H, −5H
AAAACAGp	C69H86N33O45P7	11.84	2313.36188	1155.6762	−2	1.5	−2H, −3H, −4H
UCCUUACGp	C74H95N25O59P8	11.99	2525.31028	1261.6501	−2	1.2	−2H, −3H, −4H, −5H
CCACCAUGp	C75H97N29O56P8	12.32	2547.35349	1272.6742	−2	3.1	−2H, −3H, −4H
AAAUCCUGp	C76H96N30O56P8	12.63	2572.34873	1285.1683	−2	0.3	−2H, −3H, −4H, −5H
ACAUACUGp	C76H96N30O56P8	12.63	2572.34873	1285.1683	−2	0.3	−2H, −3H, −4H, −5H
ACAUACUGp	C76H96N30O56P8	12.85	2572.34873	1285.1676	−2	−0.2	−2H, −3H, −4H
ACAUACUGp	C76H96N30O56P8	12.96	2572.34873	1285.1705	−2	2.1	−2H, −3H, −4H
CUGCCGp	C56H73N21O44P6	12.64	1929.25459	642.0863	−3	9.8	−3H
GGCGp	C39H50N18O29P4	13.37	1358.19415	1357.1889	−1	1.5	−H
CCUCACACGp	C84H109N32O63P9	13.84	2852.39477	1425.1981	−2	5	−2H, −3H, −4H, −5H
ACAUCCUCGp	C84H108N31O64P9	13.87	2853.37879	1425.6931	−2	7.1	−2H, −3H, −4H, −5H
UCACCAUCGp	C84H108N31O64P9	13.87	2853.37879	1425.6931	−2	7.1	−2H, −3H, −4H, −5H
UCACCACGp	C84H108N31O64P9	14.1	2853.37879	1425.6893	−2	4.5	−2H, −3H, −4H, −5H
AUUCUUUUGp	C83H104N25O69P9	13.93	2833.30362	1415.653	−2	5.4	−2H, −3H, −4H, −5H
ACAUCUAUUGp	C85H107N32O64P9	14.19	2878.37404	1438.1666	−2	−9.7	−2H
AUUCUUAUGp	C84H105N28O67P9	14.19	2856.33083	1427.1719	−2	9.1	−2H, −3H, −4H
UGAUGAUUCUUUUGp	C131H162N44O105P14	14.19	4464.50161	1487.1526	−3	−6.6	−3H
AUACAUUUGp	C85H106N31O65P9	14.43	2879.35805	1438.6866	−2	9.8	−2H, −3H, −5H
ACACCCUAGp	C85H109N34O62P9	14.44	2876.406	1437.2048	−2	5.8	−2H, −3H, −4H, −5H
AACAACUCGp	C86H109N36O61P9	14.72	2900.41724	1449.2093	−2	5	−2H, −3H, −4H, −5H
AAACAUCGp	C87H109N38O60P9	14.96	2924.42847	1461.2135	−2	3.9	−2H, −3H, −4H, −5H
CAAACAAAGp	C88H110N41O58P9	14.96	2947.45569	1472.7265	−2	3.5	−2H, −3H, −4H, −5H
AAAAACAUGp	C88H109N40O59P9	15.25	2948.4397	1473.2225	−2	6.2	−2H, −3H, −4H, −5H
CUGACCCUAUCAUCGp	C140H178N51O107P15	15.25	4749.61192	1582.19	−3	−5.8	−3H
UUUCACACAGp	C94H119N35O71P10	15.55	3183.41532	1590.7086	−2	4.7	−2H, −3H, −4H, −5H
UACAUAUUAGp	C95H118N36O71P10	15.84	3208.41057	1603.2007	−2	1.2	−2H, −3H, −4H, −5H
AUACAUUUGACAAAGp	C144H178N59O103P15	16.02	4845.65685	1614.2191	−3	3.1	−3H, −6H
CUACAUAAAGp	C96H120N40O68P10	16.02	3230.45377	1614.2191	−2	−0.8	−2H, −3H, −4H, −5H
GGCUGp	C48H61N20O37P5	16.02	1664.21946	1663.208	−1	−2.5	−H
UCCACUCUAUGp	C102H130N35O80P11	16.49	3465.42939	1731.7095	−2	0.8	−2H, −3H, −4H, −5H, −6H
AACAUUCUAUGp	C104H130N39O78P11	17.24	3513.45186	1755.7214	−2	1.1	−2H, −3H, −4H, −5H, −6H
AUCUUAAAAUGp	C105H130N41O77P11	17.45	3537.46309	1767.7284	−2	1.9	−2H, −3H, −4H, −5H
ACAUACUAUCAGp	C114H143N45O83P12	18.45	3841.52036	1919.7549	−2	0.6	−2H, −3H, −4H, −5H, −6H
CUGUGGp	C57H72N22O45P6	18.45	1970.24476	1969.2473	−1	5	−H
GUGGp	C39H49N17O30P4	18.55	1359.17817	1358.1705	−1	−0.3	−H
AGGGp	C40H50N20O28P4	19.39	1382.20539	690.0948	−2	−2	−2H, −H
GAGGp_1	C40H50N20O28P4	19.39	1382.20539	690.0948	−2	−2	−2H, −H
UCAUUGAGUUCUUCAAACUGp	C188H234N68O144P20	19.39	6366.78303	2121.2642	−3	3.8	−3H
UAACUACAACCAGp	C124H156N51O88P13	19.43	4169.58887	1388.8648	−3	4.8	−3H, −2H, −4H, −5H, −6H
CAGGp	C39H50N18O28P4	22.38	1342.19924	1341.1865	−1	−4.1	−H, −2H

Table 1: Tentatively identified and validated luciferase mRNA digest components within a 10 ppm mass error

based on accurate-mass matching. Cells corresponding to isomeric sequences or isobaric ions are highlighted in grey.

Figure 3 shows example data that produced an identification of digestion component UCCACUCUAUGp. This component eluted at 16.49 minutes as seen on the top left chromatogram and was identified from the *in silico* digestion library based on 5 ions carrying 2 to 6 negative charges (Figure 3, left bottom trace) at *m/z* 576.5732 ([M-6H]$^{6-}$), 692.0876 ([M-5H]$^{5-}$), 865.3603 ([M-4H]$^{4-}$), 1154.1438 ([M-3H]$^{3-}$) and 1731.7095 ([M-2H]$^{2-}$). Isotopic distributions for [M-5H]$^{5-}$ and [M-2H]$^{2-}$ ions are illustrated to show data in support of charge state assignments (Figure 3, right).
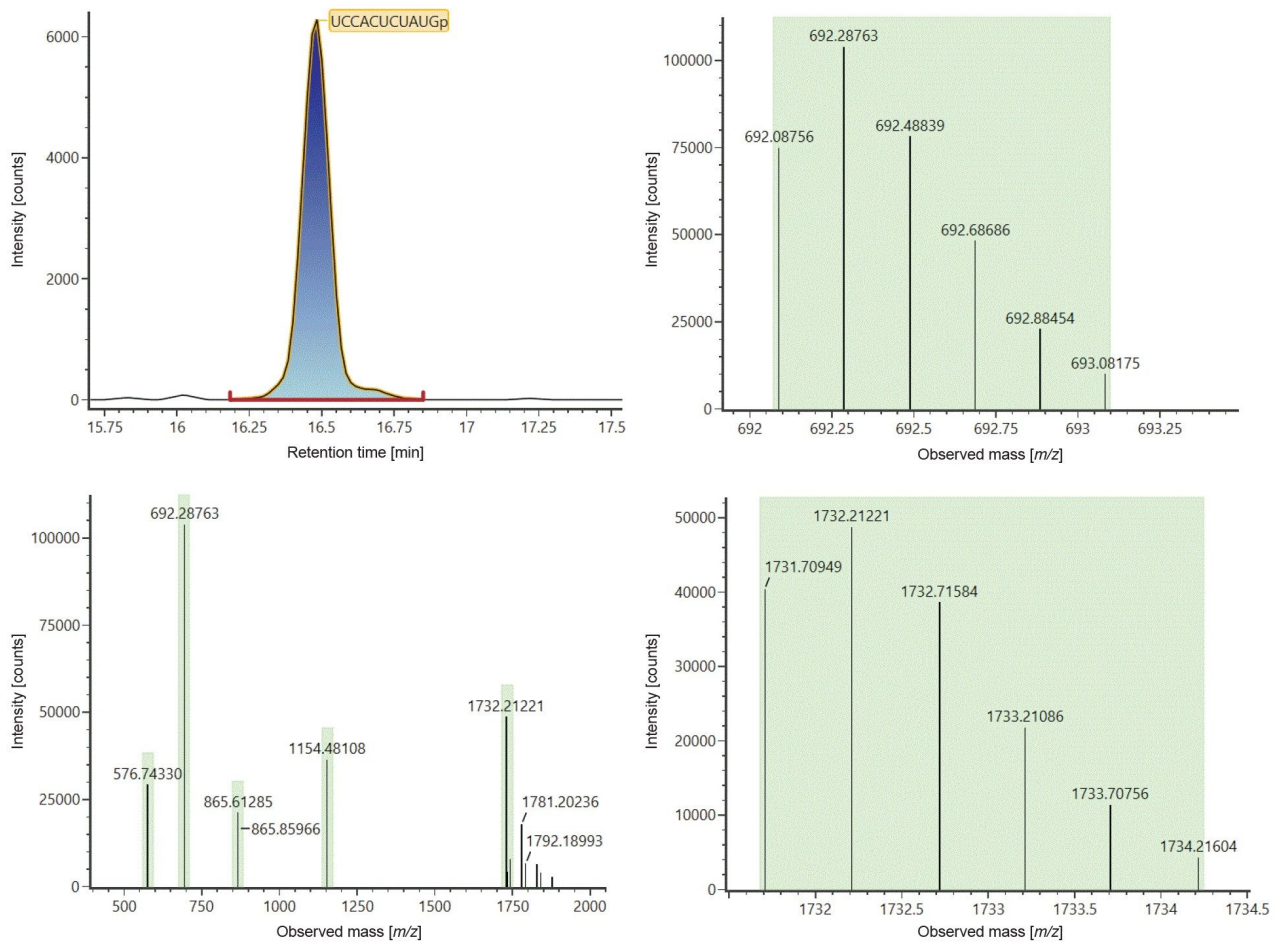
Figure 3: Identification of digest component UCCAUCACCCUGp eluting at 16.49 minutes (left top trace). The component was identified from the generated in silico digest based on 5 ions carrying 2 to 6 negative charges (left bottom trace) at m/z 576.5732 ([M-6H]$^{6-}$), 692.0876 ([M-5H]$^{5-}$), 865.3603 ([M-4H]$^{4-}$), 1154.1438 ([M-3H]$^{3-}$) and 1731.7095 ([M-2H]$^{2-}$). The experimentally observed isotopic distributions for [M-5H]$^{5-}$ and [M-2H]$^{2-}$ ions are depicted on the right top and bottom traces respectively.

Ambiguities resulting from the presence of isomeric or isobaric ions were resolved using the waters_connect CONFIRM Sequence™ application for the interpretation of MS^{E} spectra as reported in Table 2. Isomeric sequences at position 623–631 (ACAUCCUCGp) and 551–559 (UCACCAUCGp) are predicted from the RNAse T1 *in silico* digestion and both are assigned to the same retention time of 13.87 minutes. The correct assignment cannot be made using the intact mass analysis. MS^{E} data from the same injection were used to elucidate the

correct sequence for this assignment using the waters_connect™ CONFIRM Sequence application, wherein high energy fragment ions are predicted for each sequence and matched to isotope clusters of the integrated raw data via a bespoke algorithm. Confirmed fragment ions are represented on a Dot-Map allowing a rapid assessment of the sequence coverage (Figure 4, B): full sequence coverage was obtained for UCACCAUCGp such that it could be readily validated as the correct assignment (Table 2, index #63).

Neutral precursor masses obtained for manually validated digestion components (Table 1) spanned from 973.1406 Da (CCGp, RT 2.54 minutes) to a 20-mer nucleotide at 6366.7830 Da (UCAUUGAGUUCUUCAAACUGp, RT 19.39 minutes). The earliest eluting component was UGUGp, and it was identified with an observed neutral mass of 1320.1560 and a retention time of 1.64 minutes. The last luciferase mRNA digest component to elute within the manually validated set of IDs (Table 1) was CAGGp (1342.1992Da), and it was observed to elute at 22.38 minutes. Elution of CAGGp at such a late retention time was unexpected since the closely related sequence UAAGp eluted at ~4 minutes. In order to address the issue of false positives, we used the waters_connect CONFIRM Sequence application to further characterize components IDs. Validated based on MS data with MS^E data. As it can been seen in Table 2, 34/90 components, including CAGGp, did not generate an adequate number of MS^E fragments to further validate the sequence assignment, although accurate-mass matching supported the assignment. Another interesting example is the observation within the same dataset of assigned sequences AAAAACAUGUUGCCGp (4860.6678 Da, 15-mer, 9 purines) and AUACAUUUGACAAAGp (4845.6568 Da, 15-mer, 9 purines) with identical purine content but eluting 10 minutes apart. Using MS^E data, we were able to rule out AAAAACAUGUUGCCGp as a false positive and confirm the identification of AUACAUUUGACAAAGp. This demonstrates the importance of strategically using both accurate-mass matching and fragmentation spectra to aid the unambiguous identification of components resulting from digested mRNA sequences. Additionally, our observations have led us to recognize that the retention of digested mRNA components may not be as predictable as first thought and that there is an urgent need for the interactions between oligonucleotides and chromatographic stationary phases to be further studied and modeled.

Lastly, we manually estimated sequence coverage by comparing the matched, manually validated digest components to the mRNA sequence. A preliminary estimate of sequence coverage for the 401 initial matches produced a coverage value of approximately 76%. When the rigorously validated matches were checked against the mRNA sequence, a coverage value of ~22% was obtained. Many of the observed digestion components mapped to more than one location in the luciferase mRNA sequence (Table 2) and the redundancy was expected because there are only four unique residues in a modified or fully modified nucleic acid sequence.

Index	Validated luciferase mRNA digest components using accurate mass matching (10 ppm mass error)	Observed RT (min)	Position on mRNA sequence	Additional position(s) on mRNA sequence	Yes / No	coverage (%) Peak 1	Peak 2	Peak 3
						Validation using MSe data (CONFIRM Sequence)		
1	UGUGp_1	1.64	217–229	1553–1556	yes	50		
2	CCUUCGCCCGp	1.65	896–905	NA	no	0		
3	UCUACUGCGp	1.7	71–79	NA	no	0		
4	CCGGUCAAAGp	1.93	1520–1529	NA	no	10		
5	GAAGp	2.1	378–381	445–448, 635–638, 712–715	yes	25		
6	CCGp_6	2.54	59–61	246–248, 284–286, 838–840, 855–857, 1073–1075, 1076–1078, 1223–1225, 1520–1522	no	0		
7	GAGACACCCUAGp	2.54	1667–1678	NA	no	0		
8	CUCGGp	2.55	25–29	NA	no	0		
9	CUGp	2.55	177–179	422–424, 427–429, 452–454, 512–514, 560–562, 852–854, 906–908, 940–942, 965–967, 1430–1432, 1493–1495	yes	50		
10	GAGACAUCAUUGp	2.55	455–466	NA	no	16.67		
11	UAUUGAUAGCAGp	2.55	165–176	NA	no	0		
12	ACGp	2.73	779–781	809–811, 920–922, 958–960	no	0		
13	CAGp	2.73	174–176	273–275, 287–289	yes	50		
14	AUGp	2.92	209–211	291–293, 407–409, 571–573, 709–711, 806–808, 1100–1102, 1193–1195, 1271–1273, 1367–1369, 1415–1417, 1427–1429, 1467–1469, 1581–1583, 1688–1690	yes	100		
15	AAGp_4	3.18	43–45	146–148, 155–157, 379–381, 446–448, 636–638, 713–715, 1105–1107, 1139–1141, 1220–1222, 1304–1306, 1433–1435, 1475–1477, 1490–1492, 1679–1681	yes	100		
16	ACACCCUAGAAGp	3.44	1670–1681	NA	no	16.67		
17	UGAUCUUUGp	3.9	1530–1537	NA	yes	50		
18	CCCGp	3.91	902–905	NA	no	0		
19	CCUGp	3.91	1439–1442	1439–1442, 1564–1567, 1599–1602	yes	25		
20	CUCUGUGGUGp	3.91	1307–1314	NA	no	12.5		
21	GGUCCCUGp	3.91	1048–1055	NA	no	12.5		
22	AAGCCGUGp	4.17	1220–1227	NA	no	12.5		
23	UAAGp_1	4.79	644–647	1371–1374	yes	50		
24	AAAGp	5.06	312–315	1147–1150, 1645–1648	yes	100		
25	CUCUGp	5.81	1307–1311	NA	yes	60		
26	UCCCGp	5.83	1232–1236	NA	no	0		
27	CACCGp	6.18	1470–1474	NA	no	0		
28	AUCUGp	6.51	639–643	1445–1449	yes	100		
29	AUCCGp	6.53	30–34	NA	yes	20		
30	AAAAACAUGUUGCCGp	6.52	234–248	NA	no	0		
31	CAAAGp	6.79	822–826	NA	yes	40		
32	CCUCUGp	7.89	687–692	NA	yes	50		
33	CUCCCGp	7.91	968–973	NA	yes	33.33		
34	CCCCAGp	8.29	653–658	NA	no	16.67		
35	AUCCAGp	8.58	734–739	NA	yes (coelution)	33.33	33.33	
36	CAUUAGp	8.58	65–70	NA	yes	100		
37	AUUCUGp	8.63	1204–1209	NA	yes	66.67		
38	AAUCAGp	8.88	1155–1160	NA	yes	66.67		
39	UACAAGp	8.88	841–846	NA	yes	100		
40	AUCCAGp	8.89	734–739	NA	yes	33.33	33.33	
41	AACCUGp	9.03	110–115	332–337, 400–405, 984–989	yes	100		
42	ACACAGp	9.26	659–664	NA	no	16.67		
43	ACAAAGp	9.52	1025–1030	NA	yes	33.33		
44	UCUUCUGp	9.89	828–834	NA	yes	71.43		
45	AUCUCUGp	10.23	679–685	NA	no	14.29		
46	UCUACUGp	10.23	71–77	NA	yes	57.14	28.57	
47	AUUCCAGp	10.53	318–324	NA	no	14.29		
48	CAUACUGp	10.53	815–821	NA	yes	57.14		
49	AUUUCAGp	10.95	1406–1412	NA	yes	71.43		
50	AAACCUGp	11.22	1483–1489	NA	yes	71.43		
51	ACUACAGp	11.22	947–953	1285–1291	yes	71.43		
52	CCACAAGp	11.25	1557–1563	NA	yes	14.29		
53	UCUCUUCGp	11.69	1512–1519	NA	yes	37.5		
54	AAAACAGp	11.84	1197–1203	NA	yes	71.43		
55	UCCUUACGp	11.99	102–109	NA	yes	37.5		
56	CCACCAUGp	12.32	35–42	NA	yes	25		
57	AAAUCCUGp	12.63	798–805	NA	no	12.5		
58	ACAUACUGp	12.63	1277–1284	NA	yes	14.29	62.5	40
59	CUGCCGp	12.64	852–857	NA	no	0		
60	GGCGp	13.37	367–370	NA	no	0		
61	CCUCACACGp	13.84	929–937	NA	yes	22.22		
62	ACAUCCUCGp	13.87	623–631	NA	yes	33.33		
63	UCACCAUCGp	13.87	551–559	NA	yes	100	33.3	
64	AUUCUUUUGp	13.93	1418–1426	NA	yes	55.56		
65	ACAUCAUUGp	14.19	458–466	NA	yes	22.22		
66	AUUCUUAUGp	14.19	1063–1071	NA	yes	44.44		
67	UGAUGAUUCUUUUGp	14.19	1413–1426	NA	no	7.14		
68	AUACAUUUGp	14.43	1016–1024	NA	yes	55.56		
69	ACACCCUAGp	14.44	1670–1678	NA	no	11.11		
70	AACAACUCGp	14.72	740–748	NA	yes	22.22		
71	AAACAAUCGp	14.96	1162–1170	NA	yes	55.56		
72	CAAACAAAGp	14.96	665–673	NA	yes	77.78		
73	AAAAACAUGp	15.25	234–242	NA	yes	77.78		
74	CUGACCCUAUCAUCGp	15.25	512–526	NA	no	0		
75	UUUCACACAGp	15.55	1109–1118	NA	yes	80		
76	UACAUAUUAGp	15.84	1346–1355	NA	yes	80		
77	AUACAUUUGACAAAGp	16.02	1016–1030	NA	yes	20		
78	CUACAUAAAGp	16.02	1653–1662	NA	yes	50		
79	GGCUGp	16.02	420–424	NA	no	0		
80	UCCACUCUAUGp	16.49	786–796	NA	yes	72.73		
81	AACAUUCUAUGp	17.24	300–310	NA	yes	63.64		
82	AUCUUAAAAUGp	17.45	698–708	NA	yes	63.64		
83	ACAUACUAUCAGp	18.45	197–208	NA	yes	50		
84	CUGUGGp	18.45	177–182	NA	no	0		
85	GUGGp	18.55	506–509	914–917, 1312–1315	no	0		
86	AGGGp	19.39	1603–1606	NA	no	0		
87	GAGGp_1	19.39	632–635	1214–1217	no	0		
88	UCAUUGAGUUCUUCAAACUGp	19.39	593–612	NA	no	0		
89	UAACUACAACCAGp	19.43	1392–1404	NA	yes	69.23		
90	CAGGp	22.38	287–290	NA	no	0		

Table 2: Identification and validation of luciferase mRNA digest components based on accurate-mass matching

and further validation using the waters_connect CONFIRM Sequence application and collected MS^E spectra.
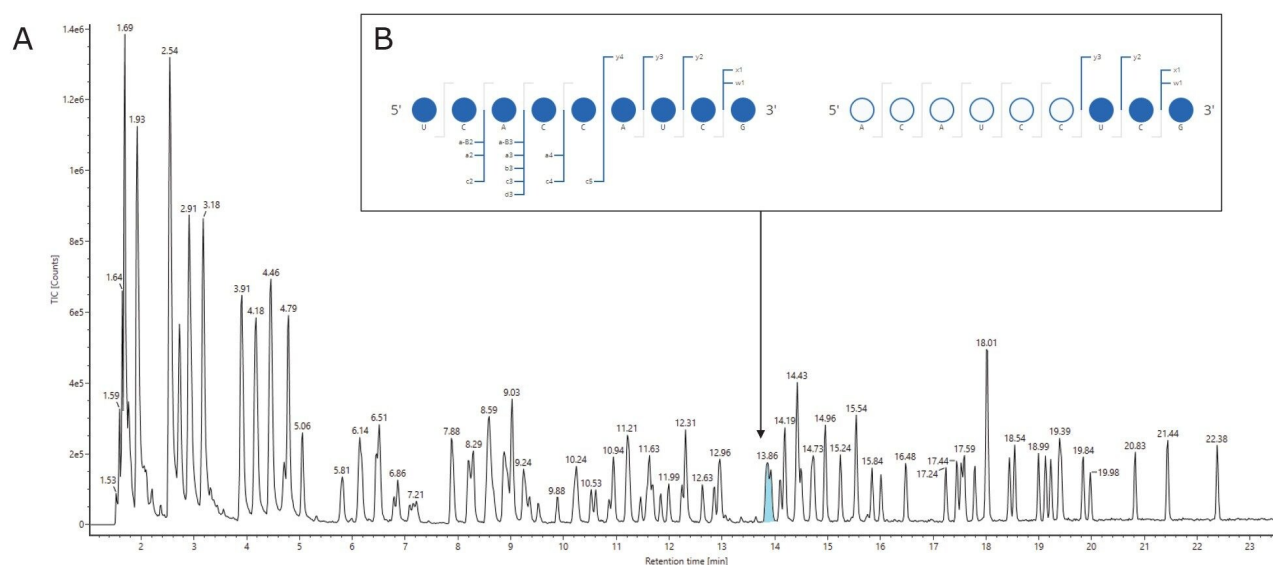

Figure 4: (A) Digested fragment components at position 623–631 (ACAUCCUCGp) and 551–559 (UCACCAUCGp) are predicted from RNAse T1 digest and are assigned to the same RT peak in the TIC. It is not possible to determine the correct assignment using intact mass information. (B) MS^E data from the same injection can be used to elucidate the correct sequence for this assignment. Using the waters_connect CONFIRM Sequence application, high energy fragment ions are predicted using McLucky annotation[11] for each sequence and matched to isotope clusters of the integrated raw data via a bespoke algorithm. The software presents confirmed fragment ions on a Dot-Map to quickly assess the sequence coverage.

Conclusion

In the present work, we established a robust analytical workflow for oligo-mapping of synthetic mRNA using IP-RPLC and MS.

- Synthetic mRNAs were reproducibly digested using RNase T1, starting with as little as 10 µg of material, and

injected without additional sample clean-up onto an ACQUITY Premier Oligonucleotide BEH C_{18} (2.1 x 150 mm, 300 Å, 1.7 μm) Column

· High chromatographic resolution was achieved using ion-pairing reversed-phase chromatography on an ACQUITY Premier LC such that digest components could be readily separated from incompletely digested mRNA and residual enzyme and efficiently detected with a BioAccord ACQUITY RDa Detector

· Annotated mRNA digest chromatograms were generated based on accurate-mass matching as facilitated by *in silico* mRNA digestion calculations and the application of waters_connect/UNIFI Scientific Libraries

· Assigned sequences for digested components were further validated based on MS^E spectra using the waters_connect CONFIRM Sequence application. In addition, Dot-Map visualization was used to quickly check the fragment ion coverage of potential assignments

With this work, it was our intent to establish the chromatographic, detection, and data interpretation approaches that would be needed to facilitate the bottom-up characterization of an mRNA molecule. RNase T1 digestion was applied only as a first example and a proof of concept on establishing a workflow for data collection and analysis. That said, there is ample opportunity to more comprehensively probe a given mRNA structure by (1) using multiple, different nucleases to generate orthogonal and additive sequence mapping information and (2) adopting a multiplexing approach for data acquisition. These aspects, aimed at achieving comprehensive sequence coverage, will be explored in future work.

References

1. Xu, S.; Yang, K.; Li, R.; Zhang, L., mRNA Vaccine Era—Mechanisms, Drug Platform and Clinical Prospection. *International Journal of Molecular Sciences* 2020, *21* (18), 6582.

2. Brenner, S.; Jacob, F.; Meselson, M., An Unstable Intermediate Carrying Information From Genes to Ribosomes for Protein Synthesis. *Nature* 1961, *190* (4776), 576–581.

3. Weide, B.; Pascolo, S.; Scheel, B. Derhovanessian, E.; Pflugfelder, A.; Eigentler, T. K. Pawelec, G.; Hoerr, I.; Rammensee, H. G.; Garbe, C., Direct Injection of Protamine-Protected Mrna: Results of a Phase 1/2 Vaccination Trial in Metastatic Melanoma Patients. *J Immunother* 2009, *32* (5), 498–507.

4. Jiang, T.; Yu, N.; Kim, J.; Murgo, J.-R.; Kissai, M.; Ravichandran, K.; Miracco, E. J.; Presnyak, V.; Hua, S., Oligonucleotide Sequence Mapping of Large Therapeutic mRNAs via Parallel Ribonuclease Digestions and LC-MS/MS. *Anal. Chem.* 2019, *91* (13), 8500–8506.

5. Plumb, R. S.; Johnson, K. A.; Rainville, P.; Smith, B. W.; Wilson, I. D.; Castro-Perez, J. M.; Nicholson, J. K., UPLC/MS[E]; A New Approach for Generating Molecular Fragment Information for Biomarker Structure Elucidation. *Rapid Communications in Mass Spectrometry* 2006, *20* (13), 1989–1994.

6. Packer, M.; Gyawali, D.; Yerabolu, R.; Schariter, J.; White, P., A Novel Mechanism for the Loss of mRNA Activity in Lipid Nanoparticle Delivery Systems. *Nat. Commun.* 2021, *12* (1), 6777.

7. Goyon, A.; Scott, B.; Kurita, K.; Maschinot, C.; Meyer, K.; Yehl, P.; Zhang, K., On-line Sequencing of CRISPR Guide RNAs and Their Impurities via the Use of Immobilized Ribonuclease Cartridges Attached to a 2D/3D-LC–MS System. *Anal. Chem.* 2021.

8. Guo, L.; Worth, A. J.; Mesaros, C.; Snyder, N. W.; Glickson, J. D.; Blair, I. A., Diisopropylethylamine/Hexafluoroisopropanol-Mediated Ion-Pairing Ultra-High-Performance Liquid Chromatography/Mass Spectrometry for Phosphate and Carboxylate Metabolite Analysis: Utility for Studying Cellular Metabolism. *Rapid Commun Mass Spectrom* 2016, *30* (16), 1835–1845.

9. Birdsall, R. E.; Gilar, M.; Shion, H.; Yu, Y. Q.; Chen, W., Reduction of Metal Adducts in Oligonucleotide Mass Spectra in Ion-Pair Reversed-Phase Chromatography/Mass Spectrometry Analysis. *Rapid Commun Mass Spectrom* 2016, *30* (14), 1667–1679.

10. Fountain, K.; Gilar, M.; Budman, Y.; Gebler, J., Purification of Dye-Labeled Oligonucleotides by Ion-Pair Reversed-Phase High-Performance Liquid Chromatography. *Journal of chromatography. B, Analytical technologies in the biomedical and life sciences* 2003, *783*, 61–72.

11. McLuckey, S. A.; Van Berkel, G. J.; Glish, G. L., Tandem Mass Spectrometry of Small, Multiply Charged Oligonucleotides. *J. Am. Soc. Mass Spectrom.* 1992, *3* (1), 60–70.

Acknowledgments

luciferase mRNA and many thoughtful discussions.

Featured Products

ACQUITY UPLC I-Class PLUS System <https://www.waters.com/134613317>

BioAccord LC-MS System for Biopharmaceuticals <https://www.waters.com/waters/nav.htm?cid=135005818>

ACQUITY UPLC Tunable UV Detector <https://www.waters.com/514228>

ACQUITY RDa Detector <https://www.waters.com/waters/nav.htm?cid=135077027>

UNIFI Scientific Information System <https://www.waters.com/134801648>

waters_connect <https://www.waters.com/waters/nav.htm?cid=135040165>

720007669, June 2022